

SUPPORTING INFORMATION

A Quantitative Nanoparticle Extraction Method for Microsecond Time Resolved Single-Particle ICP- MS Data in the Presence of High Background

Darya Mozhayeva^a and Carsten Engelhard^{a,b}*

^aUniversity of Siegen, Department of Chemistry and Biology,
Adolf-Reichwein-Str. 2, D-57076 Siegen, Germany.

^bCenter of Micro- and Nanochemistry and -Engineering, University of Siegen,
Adolf-Reichwein-Str. 2, D-57076 Siegen, Germany

*Author to whom correspondence should be addressed.

E-mail: engelhard@chemie.uni-siegen.de; Fax: +492717402041

TABLE OF CONTENTS

S-3 Size Distribution Characteristics

S-4 Figure S-1. Model histogram with labels that indicate parameters of a NPs size distribution that are used in this study to compare different extraction conditions.

S-5 Calculation of L_C and L_D for exact Poisson distribution with “well-known” BG.

S-6 Table S-1: Example calculation of y_C , critical number of gross counts, and y_D , detection limit for gross counts, for a suspension of 20 nm Ag NPs spiked with $500 \text{ ng L}^{-1} \text{ Ag}^+$.

S-7 Table S-2: Gross size detection limit (y_D) for selected ion clouds extraction conditions calculated for a suspension of 20 nm Ag NPs spiked with different concentrations of Ag^+ in solution.

S-8 Figure S-2. Average sizes of 20, 40, 60, 100 nm Ag NPs size distributions (NP suspensions in the presence of $7.5 \mu\text{g L}^{-1}$ of Ag^+) depending on different count thresholds during ion cloud extraction, T and E.

S-9 Figure S-3. Number of detected NPs for the 20, 40, 60, 100 nm Ag NPs (with $0.5 \mu\text{g L}^{-1}$ of Ag^+ in solution) depending on different count thresholds during ion cloud extraction, T and E.

S-10 Figure S-4. Number of detected NPs for the 20, 40, 60, 100 nm Ag NPs (with $7.5 \mu\text{g L}^{-1}$ of Ag^+) depending on different count thresholds during ion cloud extraction, T and E.

S-11 Figure S-5. Size starting from which the NP size distribution can be distinguished from the BG for 20 nm Ag NPs at different Ag^+ concentrations (shown on the graphs) depending on different count thresholds during ion cloud extraction, T and E.

S-12 On the Selection of the NP Suspensions Matrix

S-13 REFERENCES

Size Distribution Characteristics

The following size distribution characteristics are used in this study to describe NP size histograms and to compare the effects of extraction conditions on the final NP size distribution (Figure S-1):

- BG maximum (maximum number of extracted events in the background distribution in 2-nm bins. BG maximum is a rough indication of the quality of the ion clouds extraction process. The goal is to extract the NPs from the raw data, and not the BG. Higher number of the extracted BG counts makes the data files larger and the processing slower, also it may affect the extraction of NPs with lower sizes) (Label A in Figure 1);
- NPs average size (to determine the influence of the ion clouds extraction conditions on the obtained mean NP size) (Label B in Figure 1);
- width “W” of the size distribution that equals to two SDs of the NPs average size ($W = 2SD$, Label C in Figure 1);
- size starting from which the NP size distribution can be distinguished (if NPs are not completely separated from the BG, starting from the lowest point between the BG and the size distribution) (Label D in Figure 1);
- total number of NPs detected in the size distribution (Label E in Figure 1).

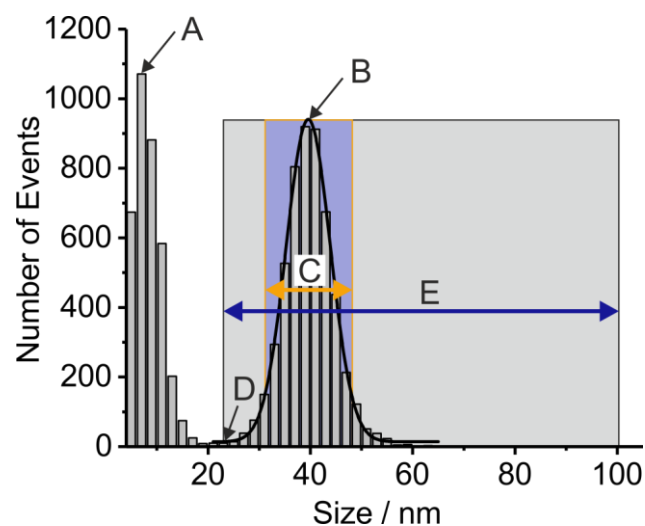


Figure S-1. Model histogram with labels that indicate parameters of a NPs size distribution that are used in this study to compare different extraction conditions: BG maximum (A), NPs average size (B), width “W” of the size distribution (C, $W = 2SD$ of the NPs average size), minimal size from which NPs can be distinguished from the BG (D), and total number detected of NPs (E).

Calculation of L_C and L_D for exact Poisson distribution with “well-known” BG

According to Currie^{1, 2}, a cumulative Poisson distribution can be used for the calculations:

$$P(y, \lambda) = \sum_{i=0}^y \frac{e^{-\lambda} \lambda^i}{i!} \quad (1)$$

The critical limit (L_C) can be expressed as:

$$P(y > y_C, \lambda = \mu_B) \leq \alpha \quad (2)$$

The detection limit (L_D) can be expressed as:

$$P(y \leq y_C, \lambda = y_D) = \beta \quad (3)$$

In formulas (2) and (3), y is the number of gross counts, μ_B is the average BG counts, α is the error of the first kind, β is the error of the second kind, y_C is the critical number of gross counts (including the BG), and y_D is the detection limit for gross counts. L_C and L_D values are net counts after BG subtraction. μ_B , y_C , and y_D may be non-integer numbers because they represent mean parameters of the Poisson distribution.

Determination of y_C and y_D can be done with the tables presented in the original publications.^{1, 2} Alternatively, an example calculation of y_C and y_D using cumulative Poisson distribution is presented in Table S-1. First, the average BG (μ_B in 25 μ s since $S = 5$) is taken, which is recalculated from the vendor software to the desired time interval. Then y_C is chosen in a way that the cumulative probability $P(y > y_C, \mu_B)$ would be below 0.05. With a known y_C (e.g. $y_C = 5$), y_D is chosen for $P(y \leq y_C, y_D)$ to be equal to 0.05 (in the example y is changing from 0 to 5). Therefore, $y_C = 5$ and $y_D = 10.51$; after BG subtraction $L_C = 2.88$, $L_D = 8.39$. For the ion cloud extraction the following parameters may be chosen if y_C and y_D are rounded: $S = 5$, $T = 10$ or 11 , and $E = 5$.

Table S-1: Example calculation of y_C , critical number of gross counts, and y_D , detection limit for gross counts, for a suspension of 20 nm Ag NPs spiked with 500 ng L⁻¹ Ag⁺ according to page S-5 descriptions.

y	μ_B in 25 μ s (S = 5)	$P_i(y, \mu_B)$	y_D	$P_i(y, y_D)$
0	2.117	0.120	10.51	2.73×10^{-5}
1	2.117	0.255	10.51	2.87×10^{-4}
2	2.117	0.270	10.51	1.51×10^{-3}
3	2.117	0.190	10.51	5.27×10^{-3}
4	2.117	0.101	10.51	0.014
5	2.117	0.043	10.51	0.029
6	2.117	0.015	10.51	0.051
7	2.117	0.005	10.51	0.077
8	2.117	1.20×10^{-3}	10.51	0.101
9	2.117	2.83×10^{-4}	10.51	0.118
10	2.117	6.00×10^{-5}	10.51	0.124
11	2.117	1.15×10^{-5}	10.51	0.118
12	2.117	2.04×10^{-6}	10.51	0.103
13	2.117	3.32×10^{-7}	10.51	0.084
14	2.117	5.02×10^{-8}	10.51	0.063
Resulting cumulative Poisson distribution probabilities, y_C , and y_D				
		$P(y > y_C, \mu_B)$ $= \sum_{i=6}^{\infty} P_i \leq 0.05$		$P(y \leq y_C, y_D)$ $= \sum_{i=0}^5 P_i = 0.05$
	y_C		y_D	
	5	0.021	10.51	0.050

Table S-2: Gross size detection limit (y_D) for selected ion clouds extraction conditions calculated for a suspension of 20 nm Ag NPs spiked with different concentrations of Ag^+ in solution.*

$C_{\text{Ag}^+} / \text{ng L}^{-1}$	T	E	μ_B / nm	y_D / nm
0	5	1	7	16
10	5	1	7	16
50	5	1	7	16
100	6	2	7	16
500	11	5	9	19
1000	15	8	10	20
2500	23	15	11	22
5000	38	28	13	24
7500	51	40	13	25

*The y_D is calculated only for selected extraction conditions based on the Table S-2. The formula $y_D = \mu_B + 3.29\sqrt{\mu_B}$ was used for the calculations, assuming normal distribution with the standard deviation of the Poisson distribution. μ_B was taken from the constructed size distributions.

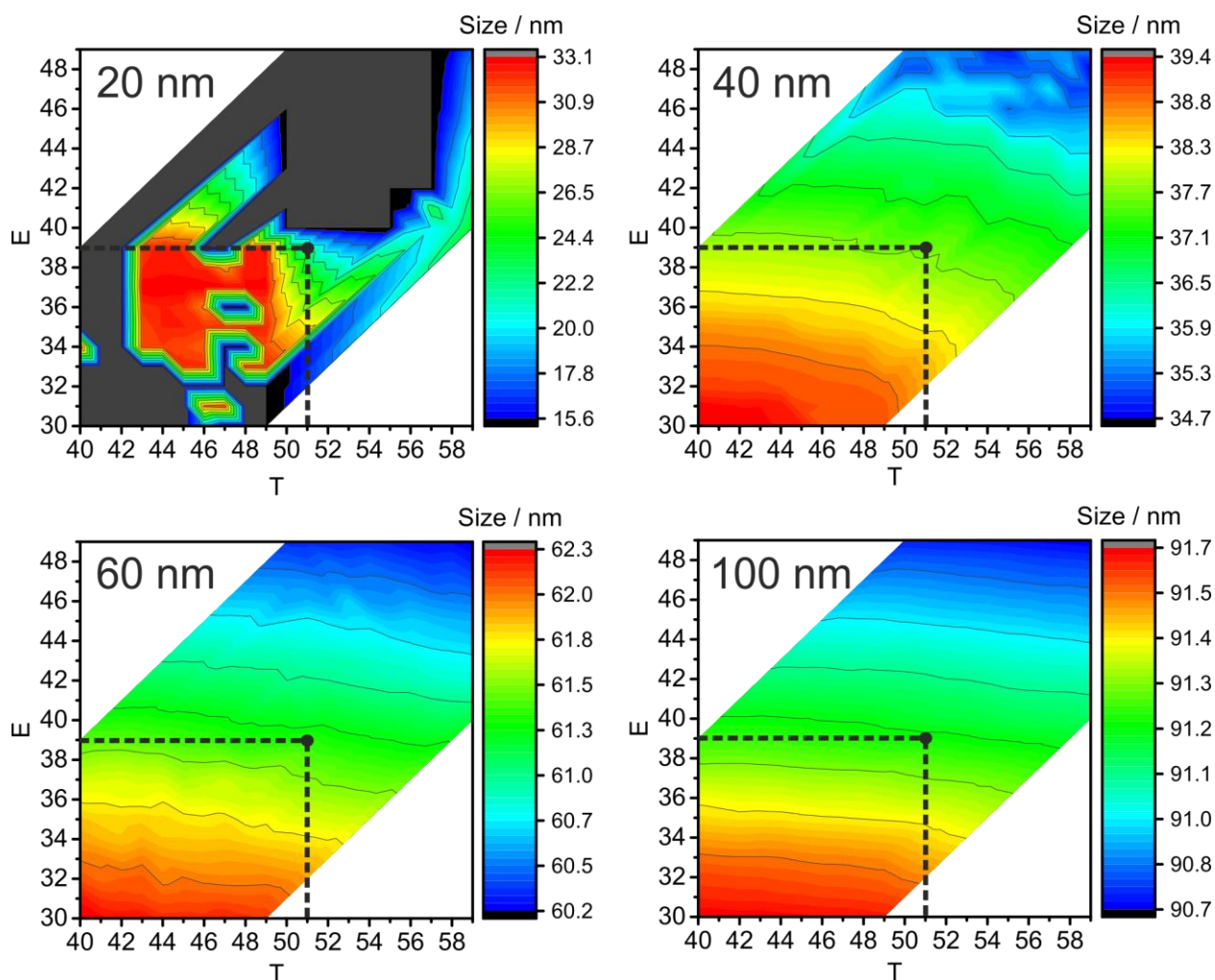


Figure S-2. Average sizes of 20, 40, 60, 100 nm Ag NPs size distributions (NP suspensions in the presence of $7.5 \mu\text{g L}^{-1}$ of Ag^+) depending on different count thresholds during ion cloud extraction, T and E. Optimal conditions ($S = 5$, $T = 51$, $E = 39$) are highlighted with black dots. Note: The step size in size resolution is for illustrative purposes only and is a result of data processing. It does not represent the actual size resolution of the SP-ICP-MS method. Also, areas of white color indicate extraction conditions, which were not tested.

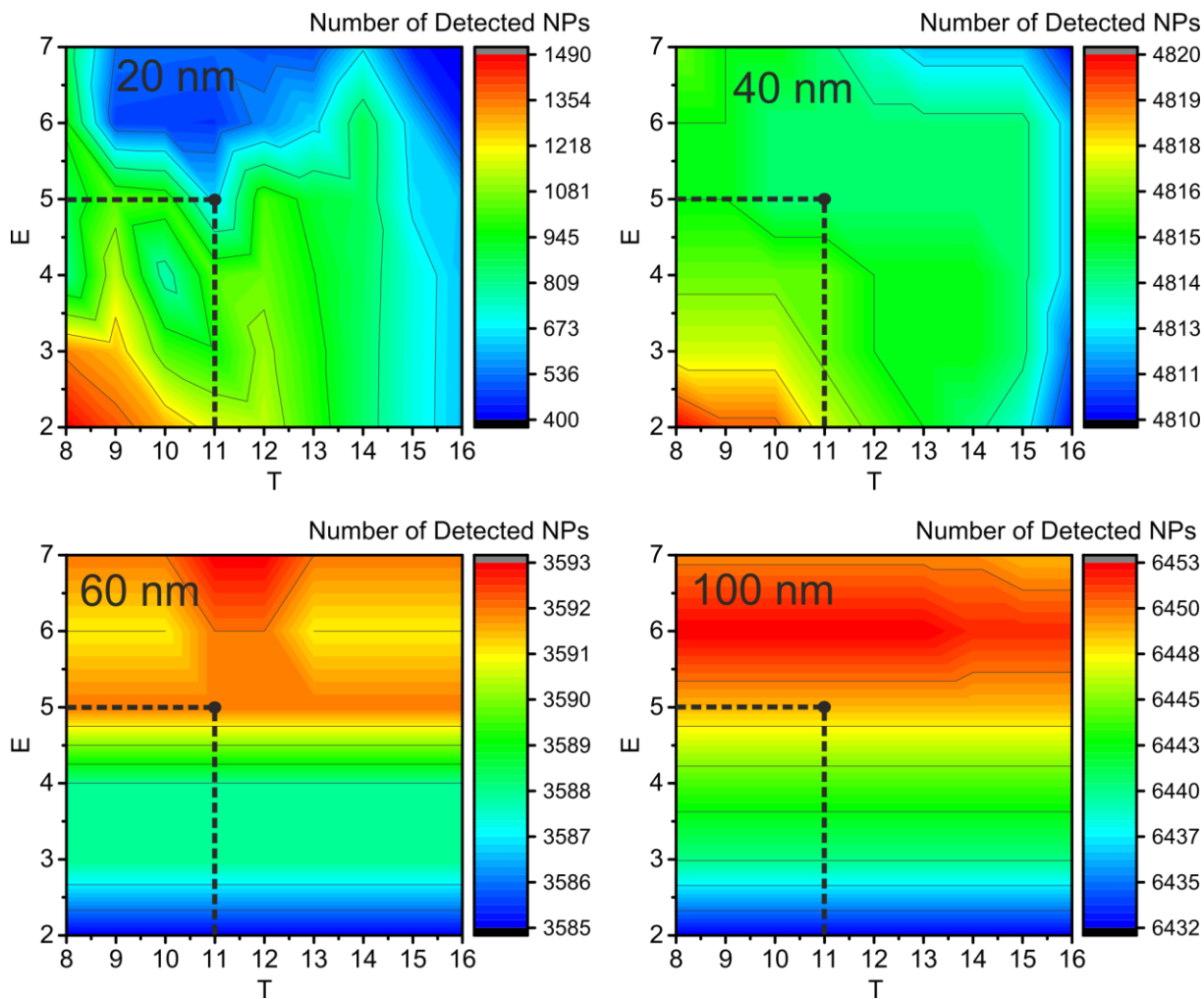


Figure S-3. Number of detected NPs for the 20, 40, 60, 100 nm Ag NPs (with $0.5 \mu\text{g L}^{-1}$ of Ag^+ in solution) depending on different count thresholds during ion cloud extraction, T and E. Optimal conditions ($S = 5$, $T = 11$, $E = 5$) are highlighted with black dots. The step size in size resolution is for illustrative purposes only and is a result of data processing. It does not represent the actual size resolution of the SP-ICP-MS method. Also, areas of white color indicate extraction conditions, which were not tested.

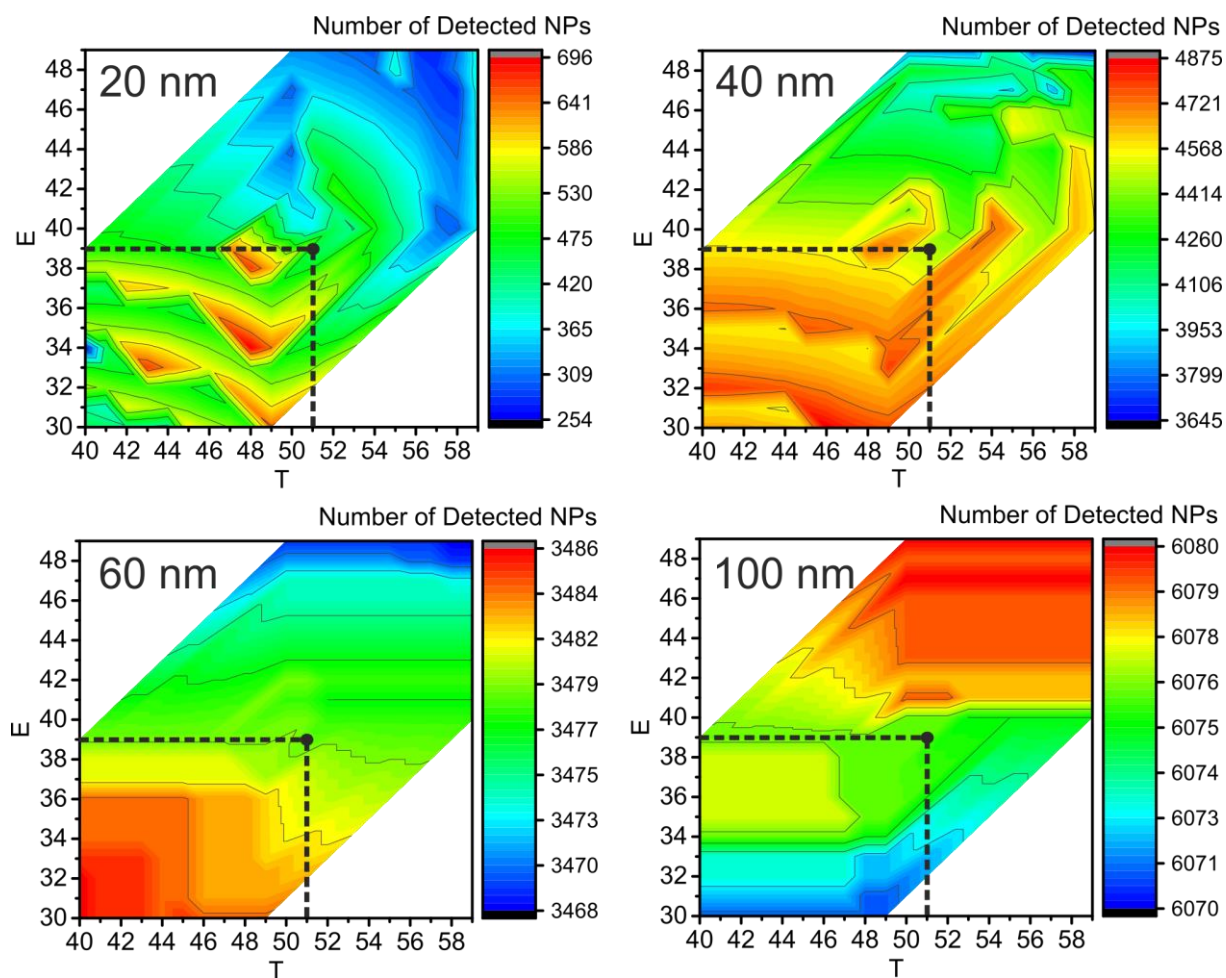


Figure S-4. Number of detected NPs for the 20, 40, 60, 100 nm Ag NPs (with $7.5 \mu\text{g L}^{-1}$ of Ag^+) depending on different count thresholds during ion cloud extraction, T and E. Optimal conditions ($S = 5$, $T = 51$, $E = 39$) are highlighted with black dots. The step size in size resolution is for illustrative purposes only and is a result of data processing. It does not represent the actual size resolution of the SP-ICP-MS method. Also, areas of white color indicate extraction conditions, which were not tested.

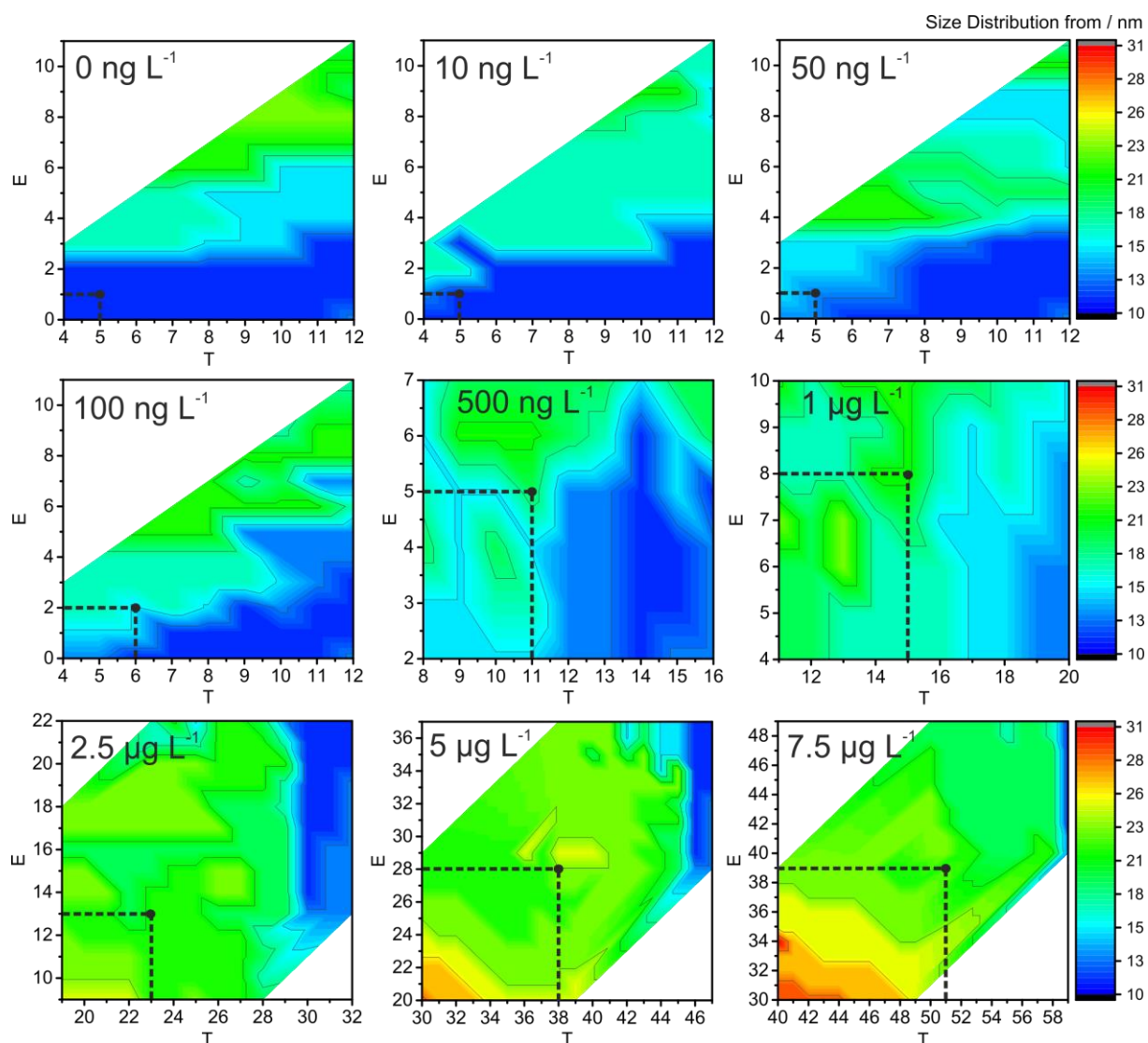


Figure S-5. Size starting from which the NP size distribution can be distinguished from the BG for 20 nm Ag NPs at different Ag^+ concentrations (shown on the graphs) depending on different count thresholds during ion cloud extraction, T and E . Optimal conditions are highlighted with black dots. The step size in size resolution is for illustrative purposes only and is a result of data processing. It does not represent the actual size resolution of the SP-ICP-MS method. Also, areas of white color indicate extraction conditions, which were not tested.

On the Selection of the NP Suspensions Matrix

When dissolved silver ions were added to the NPs suspensions in bidistilled water, it was difficult to get a stable sample nebulization (frequent interruptions of the nebulizer flow). To prevent the formation of silver hydroxide in the neutral suspension and to decrease the surface tension of the bi-distilled water (high surface tension hinders the wettability of the plastic nebulizer) HNO_3 and NaNO_3 were added to the NP suspensions as matrix modifiers. When HNO_3 or NaNO_3 were added, also nebulization became stable. It was found that the presence of 0.1% (w/v) NaNO_3 significantly decreases the apparent average size of 40 nm NPs to $86.7 \pm 2.4\%$ and 40 nm NPs with $500 \mu\text{g L}^{-1} \text{Ag}^+$ to $85.4 \pm 1.1\%$ of the original size in bidistilled water (μsDAQ) in the course of seven hours of exposure. Since sodium is an easily ionizable element, it may suppress the ionization of silver³, causing the decrease in NPs intensities. In 0.1% (w/v) HNO_3 the NPs size changed but to a lower extent to $92.7 \pm 4.6\%$ for 40 nm NPs and to $101.5 \pm 4.2\%$ for 40 nm NPs with $500 \mu\text{g L}^{-1} \text{Ag}^+$ compared to the size in bidistilled water (μsDAQ) in the course of seven hours of exposure. A lower concentration 0.025% (w/v) of HNO_3 was used further to stabilize the suspensions. Although NP size decreases up to 14% compared to the initial value in the presence of 0.025% (w/v) HNO_3 and without ionic silver in the course of seven hours, in the presence of 0.025% (w/v) HNO_3 and $1 \mu\text{g L}^{-1} \text{Ag}^+$ the size changes less than 5.4% over the course of seven hours (μsDAQ). Maximum 3.8% deviation from the initial value was detected in the intensity of $1 \mu\text{g L}^{-1} \text{Ag}^+$ in the presence of 40 nm NPs and 0.025% (w/v) HNO_3 over 7 hours after the sample preparation. Therefore, the citrate-capped NPs are stabilized in the presence of ionic silver together with traces of nitric acid, and 0.025% (w/v) HNO_3 was added to each sample in the further measurements, and the samples were analyzed not later than two hours after preparation. This set of experiments highlighted the importance of the matrix choice in SP-ICP-MS.

REFERENCES

1. L. A. Currie, *IEEE Trans. Nucl. Sci.*, 1972, **19**, 119-126.
2. L. A. Currie, *J. Radioanal. Nucl. Chem.*, 2008, **276**, 285-297.
3. J. A. Olivares and R. S. Houk, *Analytical Chemistry*, 1986, **58**, 20-25.